scientific reports

Check for updates

OPEN

Floral and pollination biology of dragon fruit reveals strategies for enhancing productivity through pollination management and reproductive window extension

Priyanka Jadhav[1], S. S. Dhumal[2], K. M. Boraiah[3]✉, Prakash Kate[3], V. D. Kakade[3], P. S. Basavaraj[3], C. B. Harisha[3], Hanamant M. Halli[3], D. B. Kshirsagar[1], B. T. Patil[1], K. K. Pal[3], S. A. Ranpise[1], K. S. Reddy[3], Jagadish Rane[4] & H. Pathak[5]

Dragon fruit (*Selenicereus undatus* (Haw.) D.R. Hunt) is emerging as a high-value crop globally. However, its reproductive biology remains poorly characterized, with conflicting reports ranging from strict self-incompatibility (allogamy) to self-compatible and autogamy. This study presents a comprehensive two-year assessment (2023 and 2024) of reproductive phenology, pollination modes, and floral biology of commercially grown white-fleshed variety (NDFW-1) that belongs to *S. undatus* (Haw.) D.R. Hunt, under subtropical Indian conditions. Flowering exhibited inter-annual variation linked to early summer rains, which acted as floral inducers—highlighting the potential of microclimate manipulation (fogging, sprinklers, rain guns) to extend the reproductive window. Although the white fleshed variety (NDFW-1) was self-compatible, manual cross-pollination significantly enhanced fruit weight, indicating limitations in natural pollination. In contrast, the red fleshed variety (NDFR-1) clone exhibited strict self-incompatibility, necessitating cross-pollination for fruit set. Anthesis dynamics and post-anthesis floral bending suggest mechanisms of delayed autogamy but are insufficient for achieving commercial-grade fruit. Pollen viability and stigma receptivity data identified a well-synchronized broader pollination window from 4 h before to 12 h after anthesis. These findings advocate precise, time-targeted pollination preferably early evening or morning hours to improve fruit set and size, particularly under rain-induced pollination deficit, and offer a validated framework for optimizing dragon fruit production in emerging regions.

Keywords Anthesis, Microclimate manipulation, Phenology, Pollination deficit, Reproductive window, Stigma receptivity

Abbreviations

CAM	Crassulacean
Acid	Metabolism
FLCL	flowering cycles
A	Anthesis
BI	Bud initiation
M	Maturity
H_2O_2	Hydrogen peroxide
BWNt	bagging with wider wire net
BNNt	bagging with narrow wire net
t ha^{-1} yr^{-1}	ton per ha per year

[1]Mahatma Phule Krishi Vidyapeeth, Rahuri, Maharashtra, India. [2]ICAR-National Research Centre on Pomegranate, Solapur, Maharashtra, India. [3]ICAR-National Institute of Abiotic Stress Management, Baramati, Maharashtra, India. [4]ICAR-Central Institute for Arid Horticulture (CIAH), Bikaner, India. [5]International Crops Research Institute for the Semi-Arid Tropics (ICRISAT), Hyderabad, India. ✉email: bors_km@yahoo.co.in

The growing awareness of the importance of a healthier diet, combined with the effects of globalization and the COVID 19 pandemic, has significantly increased the global consumption of fruits, particularly exotic fruits[1]. Among these, dragon fruit has emerged as a high-value crop owing to its nutritional richness, vibrant appearance, moderately sweet and tangy pulp with edible seeds, and diverse culinary uses[2]. Native to the tropical forests of Mexico, Central America, and South America[3], dragon fruit has recently been taxonomically reclassified as *Selenicereus undatus* (Haw.) D.R. Hunt, from its earlier designation *Hylocereus undatus* (Haworth) Britton & Rose[4,5]. As a climbing cactus with CAM-based photosynthesis, it is remarkably suited to drought-prone and high-temperature environments, making it a promising option for marginal lands[6]. Its water-retaining cladodes and shallow and dense root system enable its cultivation in resource-poor and degraded lands, such as shallow basaltic soils[7–9].

Despite the crop's long productive lifespan (20–30 years), low maintenance costs, and high returns after initial establishment[10,11], its performance in newly introduced regions including India remains inconsistent and suboptimal. Farmers in these areas report yields of only 8–10 tons per hectare per year[12], which is significantly lower than yields achieved in Vietnam[13] and other Southeast Asian countries (~ 20–35 t ha^{-1} yr^{-1}). This yield gap is largely due to the lack of region-and season-specific management practices and tailored pollination strategies. Additional challenges such as sunburn[14,15], pest and disease incidence[16–18], and high rates of flower drop during the rainy season[19,20] further exacerbate the problem. Inadequate pollination, resulting from excessive rainfall[21] and the decline of nocturnal pollinators like bats and moths[22,23], has been identified as a critical limiting factor affecting both fruit set and fruit size. Studies have shown that supplementary pollination can significantly enhance productivity and improve fruit quality in crops like strawberry[24,25], kiwifruit[26,27], and even in dragon fruit, as demonstrated in our previous studies[21].

Pollination biology in dragon fruit is complex. Most of the cultivated species exhibits heterostyly with spatial separation between stigma and anthers[28], promoting cross-pollination[29]. However, there are conflicting reports on the mode of pollination. While some studies suggest autogamy as dominant[30], others report strong xenogamy backed with self-incompatibility[31], particularly in *S. polyrhizus*. Whereas some studies[5,32] have clarified that both *S. undatus* and *S. polyrhizus* encompasses the cultivars that vary in compatibility: some are self-compatible, while others are self-incompatible and later clones require assisted pollination for successful fruit set. These discrepancies are likely due to differences in experimental conditions, species variation, environmental factors, and floral morphology. Furthermore, under natural conditions, incomplete pollination often results in reduced fruit size due to insufficient ovule fertilization, even when fruit set occurs[33,34].

Understanding floral biology—particularly the timing and synchronization of maturation of male and female reproductive organs- stigma receptivity, and pollen viability—is thus essential for designing pollination strategies based on the effective pollination window. In addition to improving pollination efficiency, extending the reproductive window to enable more and extra flowering cycles per year is another promising strategy for enhancing productivity. As a tropical species, dragon fruit's floral induction could be regulated by environmental cues rather than autonomous internal programs[35], making it highly responsive to changes in photoperiod, temperature and humidity, as earlier studies predicted[36–38]. Being a long-day plant, its production in the Northern Hemisphere is naturally seasonal, with the main harvest period broadly restricted to April–November[13] and typically observed between June and October[5] in most of the Asian countries including India. Previous research has emphasized the day length and highlighted artificial supplementary light as floral induction triggering factor during short day condition[39,40]. Despite favourable light conditions following the equinox, dragon fruit's reproductive switch is often delayed until mid-May or later in many regions across India[38]. This raises the question: what specific combination of environmental factors is necessary to initiate early flowering in the season? The present study attempts to address this by meticulously tracking floral bud initiation over two years in relation to local weather parameters. Recognizing and harnessing these natural cues could offer growers a practical means to manipulate the microclimate—to stimulate early floral initiation and could help adding an extra flowering cycle and extend the productive season to enhance annual yield.

Considering the complexities in floral biology and discrepancies in pollination affecting fruit size and yield of dragon fruit, the study was initiated to revisit existing knowledge gaps in floral and pollination biology and to develop strategies for extending the reproductive period *via* inducing early flowering and also pollination management to enhance overall yield. Specifically, the study sought to: (1) explore strategies for extending the reproductive window through floral induction based on environmental cues; (2) evaluate the necessity of supplementary pollination besides validating the mode of pollination; and (3) identify the optimal pollination window through integrated physiological and in vivo assessment of pollen viability and stigma receptivity.

Results

Reproductive behavior: reproductive period and flowering cycles

In 2023, floral bud initiation in dragon fruit was first recorded on 25th March during the first flowering cycle and last observed on 4th September in the final flowering cycle. Thus, the reproductive phase spanned a total of 5 months and 13 days during the 2023 season. However, in 2024, the reproductive phase started about 50 days later, on 13th May, and ended on 21 st September, resulting in a shorter reproductive phase of approximately 4 months and 11 days. This difference reflects a delayed start of initiation of floral bud in 2024, leading to reduction in reproductive period compared to 2023. As a result of early flowering or reproductive switching, 2023 witnessed nine flowering cycles with an extra flush or flowering cycle as a result of early or advanced flush compared to eight flowering cycles representing normal flowering pattern in 2024 (Supplementary Table 1).

The durations of important phenological phases like bud initiation to anthesis (BI-A), anthesis to maturity (A-M), and bud initiation to maturity (BI-M) were varied significantly ($p < 0.05$) across flowering cycles (FLCLs) during 2023 and 2024 (Table 1). The BI-A phase in 2023 was the longest in FLCL1 (20.95 ± 0.51 days) and the shortest in FLCL3 (17.05 ± 0.39 days). In 2024, BI-A ranged from 16.10 ± 0.31 days in FLCL3 to 22.40 ± 2.04

Flowering cycles		BI-A (Days)		A-M (Days)		BI-M (Days)	
2023	2024	2023	2024	2023	2024	2023	2024
FLCL1	-	20.95 ± 0.51^{a}	-	30.95 ± 0.22^{c}	-	51.90 ± 0.64^{c}	-
FLCL2	FLCL1	18.10 ± 0.45^{d}	18.05 ± 0.39^{e}	30.90 ± 0.31^{c}	32.00 ± 0.32^{b}	49.00 ± 0.56^{e}	50.05 ± 0.51^{b}
FLCL3	FLCL2	17.05 ± 0.39^{e}	20.95 ± 0.39^{c}	32.95 ± 0.22^{b}	29.05 ± 0.39^{e}	50.00 ± 0.46^{d}	50.00 ± 0.65^{b}
FLCL4	FLCL3	19.00 ± 0.32^{c}	16.10 ± 0.31^{f}	30.90 ± 0.31^{c}	32.90 ± 0.31^{a}	49.90 ± 0.45^{d}	49.00 ± 0.46^{c}
FLCL5	FLCL4	19.95 ± 0.39^{b}	18.00 ± 0.32^{e}	32.95 ± 0.39^{b}	30.00 ± 0.32^{d}	52.90 ± 0.55^{b}	48.00 ± 0.46^{d}
FLCL6	FLCL5	18.00 ± 0.32^{d}	21.85 ± 0.37^{b}	30.90 ± 0.31^{c}	30.95 ± 0.39^{c}	48.90 ± 0.45^{e}	52.80 ± 0.62^{a}
FLCL7	FLCL6	19.05 ± 0.39^{c}	19.00 ± 0.32^{d}	31.00 ± 0.32^{c}	31.00 ± 0.32^{c}	50.05 ± 0.60^{d}	50.00 ± 0.46^{b}
FLCL8	FLCL7	19.95 ± 0.39^{b}	19.00 ± 0.32^{d}	33.00 ± 0.32^{b}	31.00 ± 0.32^{c}	52.95 ± 0.60^{b}	50.00 ± 0.46^{b}
FLCL9	FLCL8	20.10 ± 0.31^{b}	22.40 ± 2.04^{a}	34.00 ± 0.00^{a}	30.10 ± 0.31^{d}	54.10 ± 0.31^{a}	52.50 ± 2.04^{a}
F stat		199.32**	148.01**	375.45**	250.64**	267.08**	69.40**
SE(m)		0.09	0.18	0.06	0.08	0.12	0.19

Table 1. Number of days required for initiation of bud to anthesis, anthesis to maturity and bud initiation to maturity across flowering cycles during 2023 and 2024 in white fleshed Dragon fruit. *Data followed by the same letter(s) within the same column do not differ significantly at $p < 0.01$ according to Tukey's test. BI- Bud initiation; A: Anthesis; M: Maturity or fruit ripening.

days in FLCL8. For the A-M phase, the longest duration in 2023 was recorded in FLCL9 (34.00 ± 0.00 days), while FLCL2, FLCL4, FLCL6, and FLCL7 showed shorter durations (30.90–31.00 days). However, in 2024, A-M duration was the highest in FLCL3 (32.90 ± 0.31 days) and the lowest in FLCL2 (29.05 ± 0.39 days). The total duration from BI to maturity (BI-M) was longest in the last cycles (FLCL9 and FLCL8) in both the years (54.10 ± 0.31 days in 2023 and 52.50 ± 2.04 days in 2024), while the shortest BI-M was observed in FLCL6 (48.90 ± 0.45 days) in 2023 and FLCL4 (48.00 ± 0.46 days) in 2024.

Mode of pollination

The fruit set and weight of fruits obtained in NDFW-1 (white-fleshed variety) and NDFR-1 (red-fleshed variety) upon subjecting to different pollination methods were compared (Table 2). For fruit set, NDFW-1 consistently showed high fruit set upon following most pollination methods, with 100% fruit set was achieved under manual self-pollination (MSP), manual cross-pollination (MCP), and open pollination (OP) in both the years. In contrast, NDFR-1 was able to set fruits (100%) only upon manual cross pollination. Restricted pollination methods, such as bagging with wider wire net (BWNt) and bagging with narrow wire net (BNNt), resulted in lower fruit set in both the years (Table 2). However, the fruit set under BWNt was at par with the other pollination methods. Regarding fruit weight, significant differences were observed for the variety NDFW-1, with MCP resulting in significantly highest fruit weight (588.35 g in 2023 and 587.40 g in 2024), compared to other methods. MSP resulted in an average fruit weight of 377.20 g in 2023 and 371.50 g in 2024, significantly higher than restricted pollination methods but lower than MCP. OP resulted in higher fruit weight compared to restricted pollination methods, averaging 208.35 g in 2023 and 200.20 g in 2024, but still lower than both the MCP and MSP. Restricted pollination methods, such as BWNt and BNNt, resulted in significantly lower fruit weight, with BWNt averaging 96.13 g in 2023 and 94.07 g in 2024, and BNNt averaging 68.55 g in 2023 and 67.50 g in 2024. The number of seeds per fruit also varied significantly across pollination methods. In NDFW-1, MCP produced the highest seed count per fruit (1304 in 2023 and 1355 in 2024), followed by MSP and OP, which showed moderate seed numbers. The fruit of NDFR-1 was encompassed with about 860 seeds.

Visit of insects and pollinators

Many small nocturnal insects (Blow flies -Calliphoridae) (Supplementary Fig. 2 C), beetles like European chafer (*Rhizotrogus aestivus*) (Supplementary Fig. 2 A) and Chafer beetles (*Gametis versicolor*) (Supplementary Fig. 2D) visited the flowers during 9:30 PM till 11:00 AM the next day during 6:30 AM to 8:00 AM, honey bees (*Apis cerana indica)* frequently visited and walked on flowers either for collection of pollen or nectar (Supplementary Fig. 2B).

Blooming and bending pattern: phases of anthesis and flower bending

The anthesis and flower bending behavior of white-fleshed dragon fruit variety (NDFW-1) followed a distinct sequential pattern. The pre-anthesis phase occurred between 6:00–8:00 PM (− 2 to 0 h) (Fig. 1A), marked by the initial unfurling of sepals and petals and gradual floral opening beginning around 7:00–8:00 PM (Fig. 1B), coinciding with sunset. Full anthesis was initiated at 8:00 PM (0 h) and continued until 6:00 AM (+ 10 h), with peak bloom observed between 2:00–4:00 AM (+ 6 to + 8 h) (Fig. 1C). As dawn approached (10–12 h AA), flowers began to partially close around 5:00–6:00 AM onwards (Fig. 1D), but complete closure was not observed even after 10:00 AM (Fig. 1E). Flower bending commenced only after 12 h AA, with no sign of bending between − 2 and 12 h AA (bending score: 0.00 ± 0.00). Slight bending was first noted at 14–16 h AA (1.00 ± 0.46) (Fig. 1F), followed by moderate bending at 16–18 h AA (2.10 ± 0.55) (Fig. 1G). Bending intensified significantly between 18 and 22 h AA (Fig. 1H), reaching scores of 3.05 ± 0.69 to 3.15 ± 0.49 (Fig. 1I), and culminated in complete bending by 24 h AA with a maximum score of 4.00 ± 0.00 (Fig. 1J) (Table 3).

	Fruit set (%)				Fruit weight (g)				Seeds per fruit			
	NDFW-1		NDFR-1		NDFW-1		NDFR-1		NDFW-1		NDFR-1	
Pollination method	2023	2024	2023	2024	2023	2024	2023	2024	2023	2024	2023	2024
BWNt	90.00 ± 0.31^{b}	85.00 ± 0.37^{b}	0.00 ± 0.00 ^{b}	0.00 ± 0.00^{b}	96.13 ± 13.11$^{a\#}$	94.07 ± 12.65^{a*}	NFS	NFS	279.3 ± 56.36^{ab}	285.4 ± 53.05 ^{ab}	NFS	NFS
BNNt	20.00 ± 0.41^{a}	30.00 ± 0.47^{a}	0.00 ± 0.00 ^{b}	0.00 ± 0.00^{b}	68.55 ± 7.80$^{a@}$	67.50 ± 8.50$^{a\$}$	NFS	NFS	171.0 ± 28.19^{a}	169.6 ± 31.88 ^{a}	NFS	NFS
MSP	100.00 ± 0.00 ^{b}	100.00 ± 0.00 ^{b}	0.00 ± 0.00 ^{b}	0.00 ± 0.00^{b}	377.20 ± 14.61^{c}	371.50 ± 17.94^{c}	NFS	NFS	1237.6 ± 195.32^{c}	1211.9 ± 184.16 ^{c}	NFS	NFS
MCP	100.00 ± 0.00 ^{b}	100.00 ± 0.00 ^{b}	100.00 ± 0.00 ^{a}	100.00 ± 0.00^{a}	588.35 ± 25.89^{b}	587.40 ± 26.86^{b}	296.40 ± 13.76	293.90 ± 15.72	1303.8 ± 167.48^{c}	1355.0 ± 204.65 ^{c}	859.30	860.70
OP	100.00 ± 0.00 ^{b}	100.00 ± 0.00 ^{b}	0.00 ± 0.00 ^{b}	0.00 ± 0.00^{b}	208.35 ± 58.79^{d}	200.20. ± 57.34^{d}	NFS	NFS	581.8 ± 128.03^{b}	536.8 ± 145.31^{b}	NFS	NFS
N	20				20 (except for BWNt and BNNt in both years)				10			

Table 2. Comparison of fruit set, weight and seed per fruit in white- and red-fleshed varieties under different pollination methods during 2023 and 2024. *Data followed by the same letter(s) within the same column do not differ significantly at $p < 0.01$ according to Dunn's test after subjecting to Kruskal Wallis Test; NFS: No fruit set; N = number of flowers or fruits. #, *, @ and $ represent maximum fruit set or number of samples of 18, 17, 4, 6, respectively. BWNt: Bagging with wider wire net, BNNt: bagging with narrow wire net; MSP: manual self-pollination; MCP: manual cross pollination and OP: open pollination.

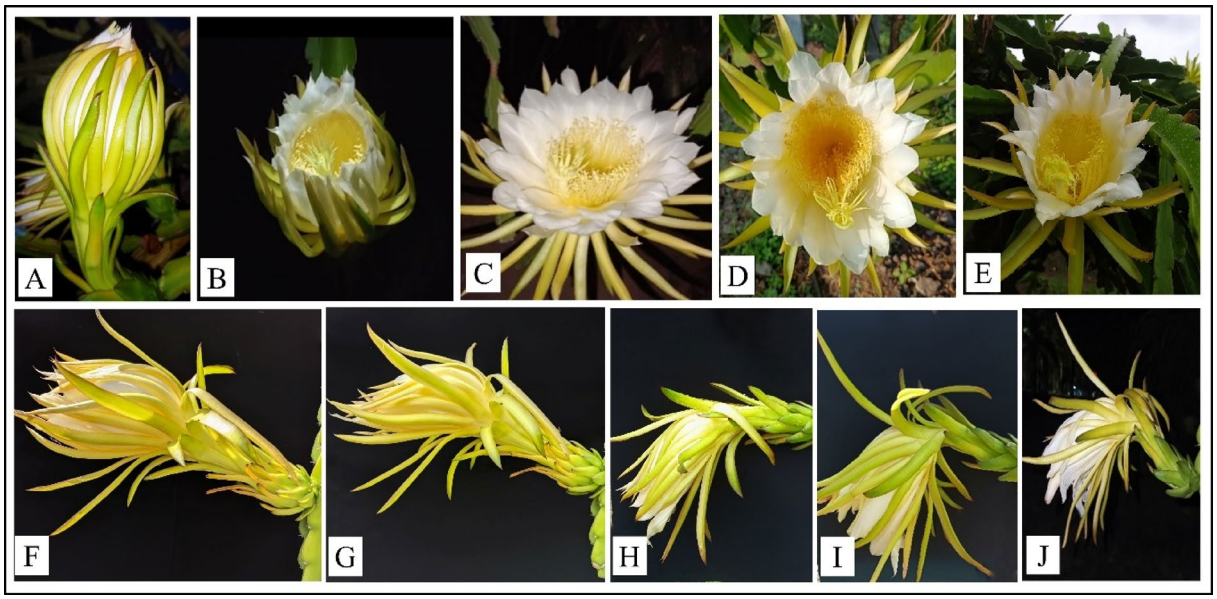

Fig. 1. Phases of anthesis or flower opening (**A**-**E**) and flower bending (**F**-**J**). Bulging of floral bud and unclasping of sepaloids indicates the initiation of anthesis between 6:00–8:00 PM (**A**); Opening of flower represents early phase of anthesis between 7:00–8:00 PM (**B**); Complete opening of flower indicates the peak anthesis phase between 2:00–5:00 AM (**C**); Flower starts closing around 5:00–6:00 AM onwards during late anthesis phase (**D**); Closing continues as sepaloids clasped on petaloids and observed only partial closing even after 10:00 AM (**E**); Loosened ball of tepaloids starts drooping around 12:00 PM (**F**); Flower bending initiated as flower desiccates around 2:00 PM (G); about 20–30% (H) and 80–90% (I) bending observed between 2:00 PM and 4:00 PM, respectively. Complete drooping of flowers with wilting signs observed between 7:00 PM and 8:00 PM (**J**).

Time interval	Bending score# (Mean ± SD)	Bending intensity	Anthesis phases
2 h BA	0.00 ± 0.00	No bending	Pre-anthesis: At the end of dusk, around 6:00 PM, the light green sepaloids of the bulged floral buds begin to unfurl. Between 6:30 and 7:30 PM, the flower starts to open gradually.
0*–2 h AA	0.00 ± 0.00	No bending	Anthesis: The unfurling of the sepaloids continues, and the flower fully opens between 8:00 and 10:00 PM. This marks the beginning of anthesis, when the male and female floral parts highly viable and receptive for effective pollination.
2–4 h AA	0.00 ± 0.00	No bending	
4–6 h AA	0.00 ± 0.00	No bending	
6–8 h AA	0.00 ± 0.00	No bending	Peak anthesis: The flower remains fully open, and all petaloids are completely unfurled.
8–10 h AA	0.00 ± 0.00	No bending	
10–12 h AA	0.00 ± 0.00	No bending	Late anthesis: At the beginning of dawn, the flower starts to close. A slow clasping of the petaloids is observed as the rays of sunlight appear.
12–14 h AA	0.15 ± 0.37	No bending	As the sun rises, the flower begins to close and is partially closed around 9:00 AM (but in red-fleshed species flower completely closes).
14–16 h AA	1.00 ± 0.46	Slight bending	
16–18 h AA	2.10 ± 0.55	Partial bending	The flower remains partially closed, and bending progresses more rapidly as sunlight intensifies and temperatures rise after noon around 4 PM.
18–20 h AA	3.05 ± 0.69	Highly bending	
20–22 h AA	3.15 ± 0.49	Highly bending	
22–24 h AA	3.80 ± 0.41	Highly bending	
24 h AA	4.00 ± 0.00	Complete bending	

Table 3. Bending intensity and anthesis phases of flower at different time interval of before and after anthesis. *: 0 h is reference anthesis time for deciding the time interval, 8:00 PM considered as anthesis time; SD: Standard deviation; number of flower tracked for monitoring bending and anthesis phases; #: scoring was done according to Boraiah et al.[63].

Physiology: anther dehiscence, viability and germination and stigma receptivity

Anther dehiscence was observed to occur between 4:30 PM -5:00 PM, as confirmed through detailed examination using a magnifying lens (Supplementary Fig. 6 F and 5G).

The pollen viability of white-fleshed dragon fruit was assessed using the acetocarmine (in-vitro) test across various time intervals during the years 2023 and 2024 (Fig. 2). Pollen viability varied significantly with time,

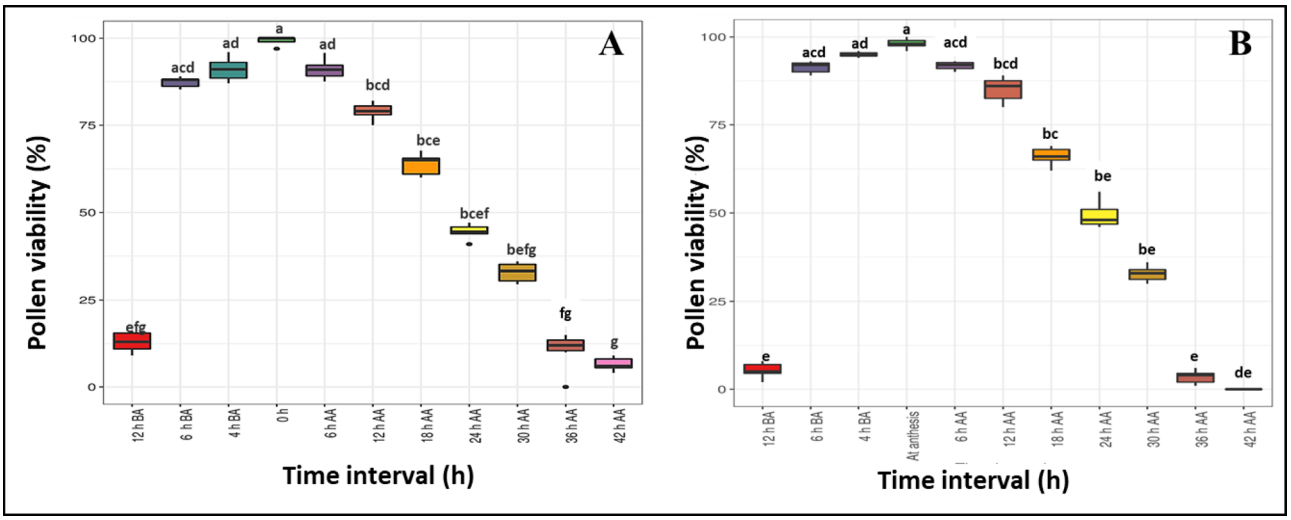

Fig. 2. The pollen viability trends over time before and after anthesis in white-fleshed variety during 2023 (**A**) and 2024 (**B**). Data analyzed statistically by Kruskal Wallis Test. Data with the same letter(s) do not differ significantly different at $p < 0.05$. The time of anthesis is designated as 0, corresponding to 8:00 PM.

Pollination time (h)	Fruit set (%)		Fruit weight (g)		Fruit length (mm)		Fruit diameter (mm)		Number of seeds per fruit	
	2023	2024	2023	2024	2023	2024	2023	2024		
−12	10 ± 0.31^{de}	0^{d}	47.50 ± 10.60^{bc}	NFS	51.00 ± 1.41^{b}	NFS	47.50 ± 3.53^{b}	NFS	57.50 ± 10.60^{bcd}	NFS
−6	65 ± 0.49^{bcf}	55 ± 0.51^{bc}	338.38 ± 10.12^{c}	344.72 ± 11.00^{c}	88.15 ± 4.89^{b}	97.27 ± 2.86^{c}	80.76 ± 2.20^{cd}	79.36 ± 2.61^{c}	872.90 ± 32.95^{bd}	875.90 ± 24.08^{cd}
−4	100 ± 0^{a}	100 ± 0^{a}	368.20 ± 13.22^{a}	376.50 ± 14.73^{a}	99.45 ± 4.27^{a}	100.65 ± 5.60^{ac}	83.75 ± 4.06^{ac}	84.40 ± 2.87^{a}	1602.30 ± 68.71^{a}	1773.40 ± 69.56^{a}
0	100 ± 0^{a}	100 ± 0^{a}	381.10 ± 14.23^{a}	383.75 ± 20.76^{a}	101.15 ± 5.93^{a}	102.10 ± 2.93^{a}	85.25 ± 2.57^{a}	85.50 ± 2.03^{a}	1712.50 ± 64.25^{a}	1844.60 ± 52.23^{a}
+6	100 ± 0^{a}	100 ± 0^{a}	372.30 ± 14.49^{a}	375.05 ± 12.76^{a}	98.55 ± 5.25^{a}	100.30 ± 4.93^{ac}	84.65 ± 2.32^{a}	83.95 ± 2.72^{a}	1729.00 ± 113.55^{a}	1761.00 ± 28.56^{a}
+12	95 ± 0.22^{af}	95 ± 0.22^{a}	367.68 ± 10.85^{a}	371.00 ± 13.68^{a}	97.26 ± 3.42^{a}	99.68 ± 3.16^{ac}	82.94 ± 2.06^{ac}	83.89 ± 2.02^{a}	1575.20 ± 131.26^{a}	1744.11 ± 48.55^{ad}
+18	85 ± 0.37^{abf}	80 ± 0.1^{ab}	232.41 ± 12.79^{bc}	246.62 ± 22.55^{bc}	86.23 ± 4.11^{b}	83.18 ± 3.71^{b}	76.52 ± 2.62^{bd}	73.62 ± 2.82^{b}	900.90 ± 53.89^{b}	878.00 ± 18.12^{bcd}
+24	60 ± 0.5^{bc}	50 ± 0.51^{bc}	136.33 ± 9.57^{b}	139.30 ± 11.91^{bc}	69.83 ± 3.21^{b}	67.10 ± 4.22^{b}	60.66 ± 2.01^{b}	56.90 ± 5.44^{b}	580.50 ± 30.37^{bcd}	227.30 ± 24.79^{bc}
+30	40 ± 0.5^{cd}	35 ± 0.5^{ce}	98.00 ± 11.83^{b}	59.00 ± 6.60^{b}	68.25 ± 2.25^{b}	32.42 ± 15.04^{b}	55.00 ± 3.02^{b}	27.57 ± 3.95^{b}	159.62 ± 26.50^{cd}	61.57 ± 8.56^{b}
+36	20 ± 0.41^{de}	10 ± 0.31^{de}	75.50 ± 3.31^{b}	47.50 ± 3.53^{bc}	58.50 ± 4.72^{b}	27.00 ± 2.82^{b}	53.75 ± 1.25^{b}	17.50 ± 3.53^{bc}	75.20 ± 42.58^{c}	47.50 ± 3.52^{bc}
+42	0^{e}	0^{d}	NFS	NFS	NFS	NFS	NFS	NFS	NFS	NFS
N	20								$N = 2–10$	

Table 4. Comparison of fruit parameters and number of seeds per fruit upon manual pollination of receptive stigma using pollens collected from different intervals of anthesis. Data analyzed statistically by Kruskal Wallis Test. Data with the same letter(s) within the same column do not differ significantly at $p < 0.05$. (-) Sign indicates time interval before anthesis; (+) Sign indicates time interval after anthesis; NFS- No Fruit Set. The time of anthesis is designated as 0, corresponding to 8:00 PM.

showing a decline as time lapsed after anthesis. In both years, the highest pollen viability was observed at 8:00 PM (0 h), with 99.28% viability in 2023 (Fig. 2A) and 98.42% in 2024 (Fig. 2B), indicating maximum viability at the time of anthesis. The pollens become viable (nearly 90%) even 6 h before anthesis (BA) and remained highly viable in the subsequent hours, with 90.97% (2023) and 92.15% (2024) at 2:00 AM (6 h after anthesis AA). These results suggested that pollen maintained higher viability throughout the 12-hour anthesis window (from 6 h before to 6 h after anthesis), with no significant differences observed at different intervals within this period, and viability levels comparable to those at the exact time of anthesis. However, as time progressed, a significant decline in viability was noted. By 12 h of post-anthesis (+12 h), the viability decreased to 79.90% (2023) and 85.57% (2024), further decreasing to 63.67% (2023) and 66.14% (2024) by 18 h (+18 h). After 24 h (+24 h), the viability dropped significantly to 44.54% (2023) and 49.38% (2024), and continued to decline further, reaching 32.90% (2023) and 32.83% (2024) at 30 h (+30 h). After 36 h (+36 h), pollen viability was very low, with 11.34% in 2023 and 3.42% in 2024, and by 42 h (+42 h), viability was nearly absent, with 5.57% (2023) and 0% (2024). The trend was evidenced with the variability in the shape or staining properties of the pollen (Supplementary Fig. 3).

Pollen viability in white-fleshed dragon fruit was also confirmed through in vivo test by comparing fruit set, as well as the weight, length, diameter, and seed number of fruits obtained from manual pollination of receptive stigmas using pollen collected at various time intervals before and after anthesis (Table 4). Pollination at anthesis

(0 h) consistently resulted in 100% fruit set in both 2023 and 2024. The fruits obtained at this time recorded the highest weight (381.10 g in 2023; 383.75 g in 2024), length (101.15 mm in 2023; 102.10 mm in 2024), diameter (85.25 mm in 2023; 85.50 mm in 2024), and number of seeds per fruit (1712.50 in 2023; 1844.60 in 2024). Pollens collected at −4 h, +6 h, and +12 h also resulted in 100%, 100%, and 95% fruit set, respectively, and produced fruits with weight, size, and seed number comparable to those obtained at 0 h. At −4 h, fruit weight was 368.20 g in 2023 and 376.50 g in 2024; at +6 h, 372.30 g in 2023 and 375.05 g in 2024; and at +12 h, 367.68 g in 2023 and 371.00 g in 2024. Seed numbers at these times also remained high, ranging from 1575 to 1744. Pollination at −6 h resulted in significantly lower fruit set (65% in 2023; 55% in 2024) and reduced fruit quality. A sharp decline in all measured traits occurred beyond +12 h, with pollens collected at +24 h and +36 h leading to poor fruit set and fruit quality. No fruit set was recorded at +42 h.

In vivo pollen germination revealed that pollen tubes began to germinate 4 h after pollination and pollen tube reached below the stigma lobes within 8 to 10 h of pollination (Fig. 3A and B). Pollens collected at −4 h (91.00%), −6 h (87.40%), and +6 h (91.40%) exhibited high and comparable germination rates (Fig. 3D and Supplementary Table 3), compared to 0 h (96.80%). Pollen collected at +12 h showed a moderately reduced germination percentage of 80.58%, though still statistically comparable in part. A noticeable decline in germination was

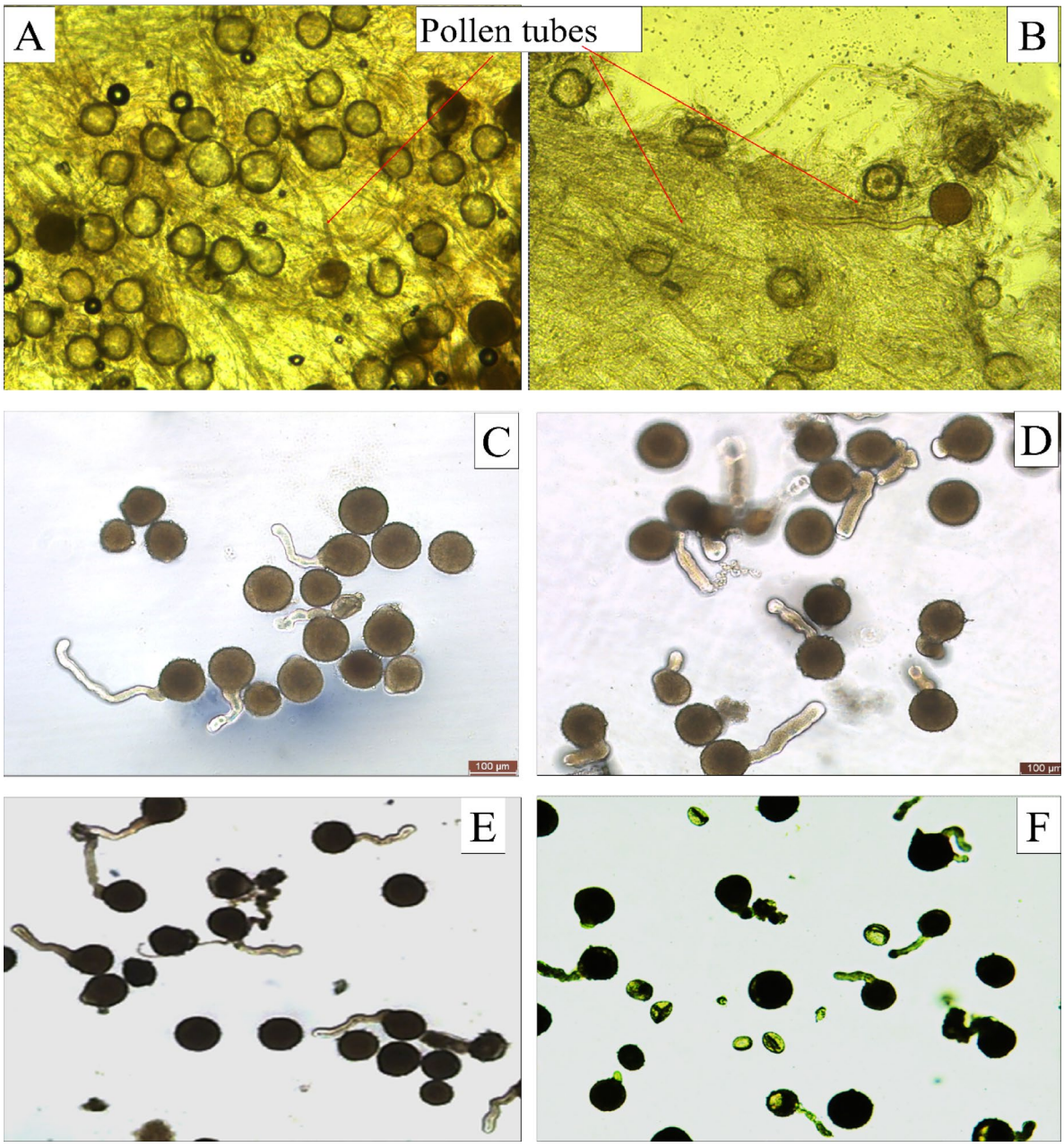

Fig. 3. In vivo pollen germination under microscope (**A**) & (**B**) red arrow indicate pollen tube growth on stigma lobes. In vitro pollen germination at −12 h (**C**), at anthesis (**D**), +24 h (E) and +36 h (F).

observed at + 18 h (74.66%), which further dropped sharply reduced to 40.66% (Fig. 3E) and 22.40% (Fig. 3F) at + 24 h and + 36 h, respectively. The lowest germination (8.2%) was recorded at −12 h (Fig. 3C).

The stigma receptivity based on the hydrogen peroxide (H_2O_2) test (in vitro), revealed a clear pattern of varying receptivity across different time intervals before and after anthesis (Supplementary Table 4). Stigma receptivity was absent at 48 h before anthesis (Fig. 4A) and appeared at a very low level (+) at 42 h before anthesis. It increased to low (++) at 36 h before anthesis, moderate (+++) at 30 h before anthesis, and high (++++) at 24 and 18 h before anthesis (Fig. 4B). Very high receptivity (+++++) was observed from 12 h before anthesis through 12 h after anthesis (Fig. 4D), including at the time of anthesis (0 h) (Fig. 4C). Receptivity then decreased to high (++++) at 18 h after anthesis, moderate (+++) at 24 h after anthesis (Fig. 4E), low (++) at 30 h after anthesis, and very low (+) at 36 h after anthesis. No receptivity was recorded at 42 and 48 h after anthesis (Fig. 4F).

The stigma receptivity was further confirmed by comparing weight, length, and diameter of fruits obtained through manual pollination of stigma at (0 h), before (- h) and after (+ h) anthesis using viable pollen (Table 5). Pollination at anthesis (0 h) consistently resulted in 100% fruit set in both 2023 and 2024, with the highest fruit weight (381.55 g in 2023; 393.90 g in 2024), length (99.65 mm in 2023; 100.60 mm in 2024), and diameter (88.85 mm in 2023; 87.60 mm in 2024). Pollination at − 4 h, − 6 h and − 12 h also led to 100% fruit set and produced fruits with weight and size comparable to those at 0 h. At − 18 h, although fruit set remained high (95%), fruit weight and size declined significantly, and this trend became more pronounced at − 24 h and − 30 h, where fruit set remained moderate to high (80% and 70–75%, respectively), but fruit traits showed a noticeable reduction. Beyond − 30 h, both fruit set and fruit quality declined sharply, with no fruit set recorded at − 54 h. Similarly, after anthesis, pollination at + 6 h and + 12 h resulted in 100% fruit set and fruit traits at par with those obtained at 0 h. At + 18 h, fruit set remained high (95%), but fruit weight and size decreased significantly. Further decline was observed at + 24 h (75–80% fruit set), where quality parameters of fruit were lower than earlier intervals. Beyond + 24 h, fruit set and fruit traits deteriorated sharply, with no fruit set recorded at + 42 h.

Discussion

The present study provides a comprehensive assessment of reproductive phenology, pollination biology, and efficiency in *S. undatus* (white-fleshed dragon fruit) under subtropical Indian conditions over two consecutive years (2023 and 2024). The findings offer valuable insights into strategies for improving productivity and reproductive success through informed manipulation of flowering and pollination windows.

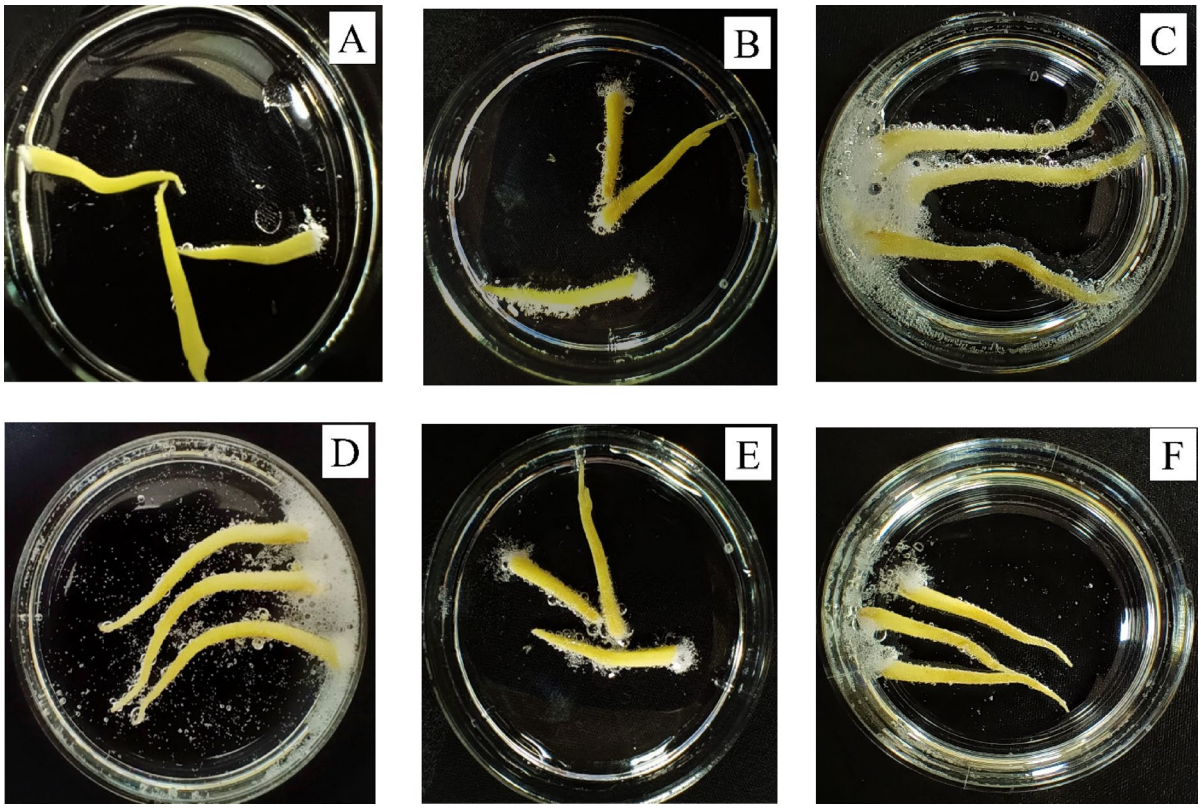

Fig. 4. The receptivity (In vitro: Hydrogen peroxide test) of stigma at 48 h BA (**A**), 24 h BA (**B**), anthesis (**C**), 12 h AA (**D**), 24 h AA (**E**), and 48 h AA (**F**). The bubble intensity in each time zone indicates the relative receptivity of stigma. More the bubbles more the receptive of stigma and vice versa. The time zone before the anthesis is represented as BA whereas after the anthesis is represented as AA.

	Fruit set (%)		Fruit weight (g)		Fruit length (mm)		Fruit diameter (mm)	
Time interval	2023	2024	2023	2024	2023	2024	2023	2024
−54	0^{f}	0^{g}	NFS	NFS	NFS	NFS	NFS	NFS
−48	30 ± 0.47^{e}	25 ± 0.44^{fg}	66.16 ± 1.94^{cd}	68.40 ± 2.07^{ef}	56.33 ± 1.96^{de}	58.80 ± 4.14^{de}	46.16 ± 1.16^{de}	45.60 ± 2.07^{e}
−42	45 ± 0.51^{de}	35 ± 0.49^{ef}	79.55 ± 2.29^{cd}	70.28 ± 12.85^{ef}	62.66 ± 2.23^{de}	60.57 ± 4.19^{e}	52.88 ± 5.06^{de}	51.85 ± 1.77^{e}
−36	65 ± 0.49^{cd}	60 ± 0.5^{cde}	87.61 ± 4.21^{cd}	108.08 ± 13.02^{ef}	64.69 ± 3.06^{de}	71.75 ± 2.41^{de}	57.53 ± 4.23^{de}	61.33 ± 1.61^{e}
−30	75 ± 0.44^{abc}	70 ± 0.44^{abc}	113.33 ± 6.09^{cd}	144.07 ± 7.59^{def}	75.40 ± 4.70^{bcd}	78.00 ± 2.85^{bcde}	65.06 ± 2.15^{bcd}	67.14 ± 3.15^{cde}
−24	80 ± 0.41^{abc}	80 ± 0.41^{abc}	126.62 ± 6.20^{bc}	208.25 ± 17.96^{cd}	80.00 ± 2.16^{bc}	81.25 ± 2.97^{bcd}	68.56 ± 2.22^{bc}	69.81 ± 2.00^{bcd}
−18	95 ± 0.22^{ab}	90 ± 0.31^{ab}	228.68 ± 12.99^{b}	252.00 ± 17.49^{c}	84.31 ± 3.49^{b}	87.50 ± 2.55^{b}	71.94 ± 2.19^{b}	73.88 ± 6.43^{bc}
−12	100 ± 0^{a}	100 ± 0^{a}	343.10 ± 17.56^{a}	374.80 ± 23.42^{ab}	95.75 ± 2.88^{a}	96.85 ± 3.34^{a}	85.75 ± 3.40^{a}	85.30 ± 2.25^{a}
−6	100 ± 0^{a}	100 ± 0^{a}	375.50 ± 22.54^{a}	377.80 ± 8.01^{a}	98.45 ± 2.08^{a}	97.65 ± 2.70^{a}	86.00 ± 3.02^{a}	85.90 ± 1.94^{a}
−4	100 ± 0^{a}	100 ± 0^{a}	378.55 ± 9.01^{a}	386.70 ± 9.87^{a}	98.90 ± 2.70^{a}	98.00 ± 4.91^{a}	87.50 ± 2.74^{a}	86.50 ± 3.83^{a}
0	100 ± 0^{a}	100 ± 0^{a}	381.55 ± 36.44^{a}	393.90 ± 23.76^{a}	99.65 ± 2.70^{a}	100.60 ± 3.10^{a}	88.85 ± 2.13^{a}	87.60 ± 1.81^{a}
+6	100 ± 0^{a}	100 ± 0^{a}	373.55 ± 23.09^{a}	380.15 ± 11.27^{a}	98.55 ± 3.85^{a}	97.40 ± 3.25^{a}	86.05 ± 2.25^{a}	86.10 ± 1.94^{a}
+12	100 ± 0^{a}	100 ± 0^{a}	341.70 ± 16.90^{a}	376.45 ± 9.24^{a}	96.85 ± 4.12^{a}	96.80 ± 3.54^{a}	85.80 ± 1.76^{a}	84.80 ± 2.37^{a}
+18	95 ± 0.22^{ab}	95 ± 0.22^{a}	236.10 ± 16.87^{b}	254.05 ± 23.6^{c}	84.73 ± 3.31^{b}	86.84 ± 5.29^{bc}	72.57 ± 1.95^{b}	77.36 ± 2.47^{b}
+24	80 ± 0.41^{abc}	75 ± 0.44^{abc}	130.62 ± 16.61^{bc}	187.60 ± 12.82^{cde}	72.68 ± 2.72^{cde}	78.00 ± 3.58^{cde}	61.87 ± 3.00^{cde}	65.60 ± 2.64^{de}
+30	70 ± 0.47^{bcd}	65 ± 0.49^{bcd}	88.64 ± 8.14^{cd}	147.53 ± 8.81^{def}	67.71 ± 3.45^{cde}	74.53 ± 3.30^{de}	56.42 ± 7.24^{de}	64.69 ± 2.13^{de}
+36	45 ± 0.51^{de}	40 ± 0.5^{def}	57.55 ± 1.94^{d}	73.625 ± 5.15^{f}	48.55 ± 2.87^{e}	52.75 ± 3.10^{e}	40.88 ± 1.76^{e}	62.75 ± 2.25^{de}
+42	0^{f}	0^{g}	NFS	NFS	NFS	NFS	NFS	NFS

Table 5. Comparison of fruit parameters upon manual pollination of the stigma at different intervals of anthesis using viable pollens. Data analyzed statistically by Kruskal Wallis Test. Data with the same letter(s) within the same column do not differ significantly at $p < 0.05$. (-) Sign indicates time interval before anthesis; (+) Sign indicates time interval after anthesis. The time of anthesis is designated as 0, corresponding to 8:00 PM.

Temporal patterns of floral initiation showed significant inter-annual variation. In 2023, flowering began in late March and continued through early September, lasting approximately 5.5 months. During this period, nine distinct flowering cycles were recorded (Supplementary Fig. 5). In contrast, the 2024 season exhibited a delayed onset in mid-May and concluded by the third week of September. This shortened the reproductive window to around 4.5 months and reduced the number of cycles to eight. This discrepancy was closely linked to environmental triggers. Notably, early flower initiation in 2023 coincided with unseasonal summer rains around the March equinox, resulting in cooler temperatures and elevated humidity (Supplementary Fig. 4). This suggests that early pre-monsoon rainfall may act as a floral inducer in *S. undatus*, a phenomenon previously reported in southern India[38] and comparable to "mango showers" known to stimulate flowering in crops like coffee[41]. These findings strongly suggested that dragon fruit is a photo-thermo-sensitive fruit crop, responsive to the combined effects of increasing day-length, moderate temperatures, and elevated humidity aligned with comprehensive observation of Wilkie et al.[35].. While prior studies emphasized photoperiod and monsoonal influence[38–40], our findings identify early summer rainfall during periods of long days as a critical and previously underappreciated cue for advancing floral initiation. These insights pave the way for developing targeted microclimate manipulation strategies—such as misting, fogging, or deploying rain guns—to recreate favourable pre-monsoon conditions, thereby advancing floral initiation, extending the reproductive window, and potentially enabling an additional flowering cycle to boost overall yield.

Supplemental data from 2025 further support this hypothesis. The fairly sufficient and continuous rainfall observed in first week of April with first measurable rainfall of 5.2 mm on April 3rd - the earliest precipitation event (Supplementary Table 2) of the season in Karnataka—closely followed by visible floral bud initiation within 2–3 days (supplementary Fig. 8). This strongly implies that the initial rainfall acts as a trigger, likely by lowering ambient temperatures and triggering the floral transition, thereby activating reproductive pathways. In contrast, at the experimental site, despite two isolated rain events in early April, first floral bud initiation was only observed around last week of May, suggesting a possible rainfall threshold required to initiate the floral pathway via moderating the summer harsh weather. These insights suggest that integrating early rainfall monitoring with photoperiod data could enhance the precision of flowering cycle predictions, offering practical implications for orchard management and yield optimization. However, further systematic validation involving multiple locations and additional weather parameters beyond rainfall, such as temperature, humidity, and solar radiation, is necessary to comprehensively understand the environmental controls on floral induction. Future experiments incorporating these variables will help to strengthen and generalize these findings. Phenological monitoring revealed that the durations from bud initiation to anthesis (BI-A), anthesis to maturity (A-M), and full bud-to-maturity (BI-M) remained consistent across years and closely aligned with previous observations[42–44]. Our findings further corroborate reports from Marques et al.[45]. and Castillo and Ortiz[46], who noted full-cycle durations of 50–60 days. However, extended durations in later flowering cycles likely reflect seasonal transitions and resource constraints, with variability potentially attributed to shifts in day-length, temperature, and humidity[47].

The reproductive behaviour of NDFW-1 (white-fleshed) and NDFR-1 (red-fleshed) varieties revealed contrasting pollination strategies with significant implications for specific pollination management. NDFW-1 demonstrated clear self-compatibility, with 100% fruit set achieved under manual self-pollination (MSP), manual cross-pollination (MCP), and open pollination (OP). These results support previous findings that some *S. undatus* accessions are autogamous[33]. Despite consistent fruit set, substantial differences in fruit weight were observed: MCP produced significantly larger fruits (~ 588 g) compared to MSP (~ 374 g) and OP (~ 204 g) (Table 2), indicating that while self- and open pollination suffice for fruit initiation, they often result in suboptimal fertilization and inadequate seed development. This is particularly relevant in multi-ovule berry fruits like dragon fruit, where complete fertilization is necessary for full fruit development[48,49].

In contrast, the NDFR-1 clone, likely representing *S. polyrhizus*, was completely self-incompatible, setting fruit only under MCP. No fruit was produced via MSP or OP despite the presence of viable pollen, suggesting a genetically regulated self-incompatibility system, as reported in other *Selenicereuss* species[5,50–52]. These findings underscore the broad diversity of reproductive strategies across *Selenicereus* spp. and the importance of understanding cultivar-specific pollination biology for effective breeding and cultivation strategies.

Pollination exclusion experiments using bagging treatments further elucidated pollination modes. NDFW-1 showed 85–90% fruit set under wide mesh (BWNt) treatments permitting wind pollination, but fruits were significantly smaller (~ 95 g). Under narrow mesh (BNNt), which restricted both wind and insect access, fruit set declined to 20–30%, and fruit weight dropped to ~ 67 g (Table 2). These results suggest that minimal pollen transfer can initiate fruiting, but to achieve high-quality fruit with better fruit weight or size, efficient manual pollination is essential, as fruit size is closely associated with the number of seeds per fruit. Traditional nocturnal pollinators such as bats and moths[53] were rarely observed, possibly due to regional variation. Instead, visits from nocturnal beetles (*Gametis versicolor*), blowflies, and early morning foragers like *Apis cerana indica* were more common, though their pollination efficacy remains uncertain. Pronounced heterostyly and spatial separation between anthers and stigmas (Supplementary Fig. 2), as noted by Weiss et al.[33], may impede effective pollen transfer, necessitate supplementary manual or assisted pollination to ensure both fruit set and fruit quality.

Floral phenology of white-fleshed type (*S. undatus*) exhibited adaptive traits likely contributing to reproductive assurance. The onset of anthesis in our study began around 6:00–6:30 PM, in synchrony with local sunset, earlier than previously reported[32,42,54]. Full anthesis extended through the night (8:00 PM–6:00 AM), peaking between 2:00 and 5:00 AM. Notably, flowers remained partially open in the morning, even after 10:00 AM, despite earlier reports stating that they begin closing around 7.00 AM[37] and completely closed at around midday[28] in red-fleshed clones. Such prolonged floral openness not only limit the closure movement of stigma and anthers and also expose flowers to adverse weather, particularly rain, leading to pollen washout and reduced fertilization success—a hypothesis supported by lower fruit weight and seed set (Table 2) observed under natural pollination which is providing stronger evidence for our earlier observation[21]. Thus, although anthesis timing may represent an evolutionary strategy to broaden pollinator access, it simultaneously introduces vulnerabilities that reduce reproductive efficiency under cultivation. In white-fleshed variety (NDFW-1) of *S. undatus*, flowers initiated bending approximately 14 h after anthesis and completed the movement within 24 h. This sequential post-anthesis floral bending, documented in the present study, constitutes a novel observation of ecological relevance and, to our knowledge, represents the first report of this phenomenon irrespective of species. This bending pattern may bring both the sexual floral parts (stigma and anthers) closure and reduce heterostylous separation and facilitate delayed autogamy in the absence of effective pollinators, a mechanism observed in other heterostylous or outcrossing species as a form of reproductive assurance[33,55]. However, while this may safeguard against complete reproductive failure assuring fruit set, but the resulting fruit quality remains inferior to those obtained via cross-pollination, emphasizing the need for assisted pollination to maximize yield.

Physiological assessment of pollen and stigma function further delineated a critical pollination window. Anther dehiscence occurred between 4:30 and 5:00 PM—prior to anthesis—confirming earlier findings[32], and indicating that viable pollen is available before floral opening. The present study established a clear temporal pattern of pollen viability (acetocarmine test) in *S. undatus*, peaking at anthesis (0 h) with over 98% viability and remaining above 90% from − 6 h to + 6 h, as confirmed by in-vitro germination. In vitro germination ranged from 87% to 96% within this window, significantly exceeding rates reported by Li et al.[48].. However, from a commercial point of view (based on in-vivo test), the pollen becomes viable after anther dehiscence (−4h) contrasting with delayed viability reported by Del Angel-Perez et al.[56]., and aligning partially with findings from Boraiah et al.[54]. and Weiss et al.[33].. The consistency between indirect viability tests and in vivo outcomes confirms a synchronized reproductive window, with optimal pollination occurring between − 4 h and + 12 h, and peak efficacy between 0 h and + 6 h (Fig. 5A), underscoring the need to validate viability tests through actual fruit set data (in-vivo test).

Similarly, H_2O_2 test revealed that stigmas of *S. undatus*, were very highly receptive (+++++) between − 12 h and + 12 h as more and intense bubbles were observed, aligning with maximum fruit set and superior fruit traits in in-vivo test. Pollination during this peak, results in the highest fruit quality, with fruit weight exceeding the fruits obtained under natural or open pollination (Table 2) and comparable to anthesis-pollinated fruits (Table 5). These findings, consistent with Li et al.[48,49], emphasize that the stigmas between − 12 h and + 12 h were receptive enough to produce commercial grade fruits with a peak between − 4 h and + 6 h, highlighting the critical role of precise pollination timing.

Overall, while stigma receptivity extends from − 12 h to + 12 h (Fig. 5B), the narrower functional viability of pollen from − 4 h to + 12 h (Fig. 5A) defines a practical 18-hour effective pollination window for maximizing fruit quality. Pollen collected before − 4 h remains largely immature and non-viable due to incomplete dehiscence, limiting its fertilization potential. Hence, manual pollination performed within this − 4 h to + 12 h window reliably results in 100% fruit set and consistently high fruit weight, outperforming open-pollinated fruit (Table 2). Notably, this window is broader than those observed in crops such as apricot[57], pear[58], and even

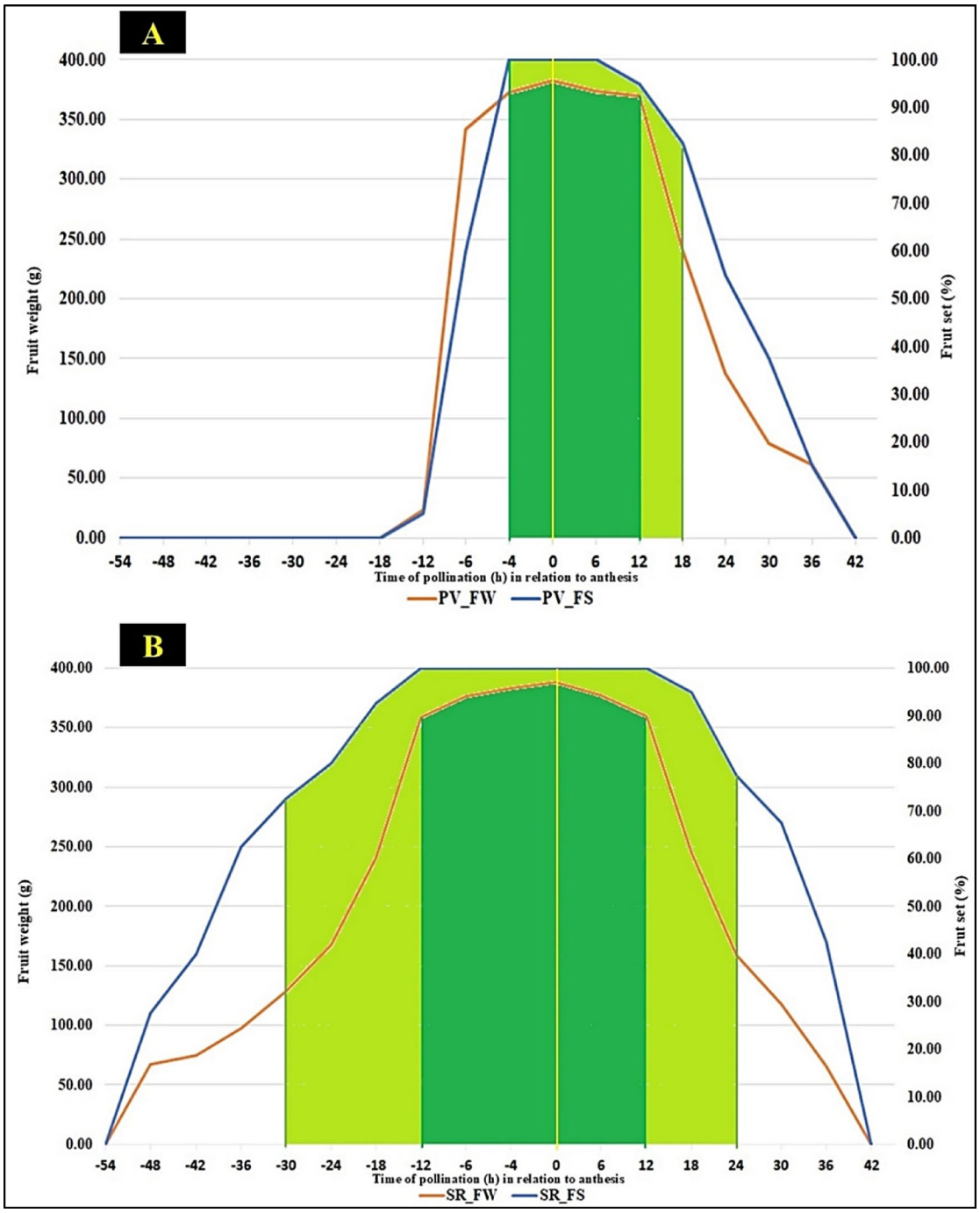

Fig. 5. Effective pollination zone based on the pollen viability (A) and stigma receptivity (B). The figures illustrate fruit set and fruit weight resulting from pollination (using variable pollen or stigma) between 54 h before anthesis (−54) and 42 h after anthesis. The time of anthesis is designated as 0, corresponding to 8:00 PM. The blue line represents fruit set, and the orange line represents fruit weight. The time intervals during which pollination resulted in fruit set and fruit weight comparable to those achieved at anthesis considered as effective pollination zones. Accordingly, the effective zone for fruit set and fruit weight represented in light and dark green area respectively.

other dragon fruit cultivars[48], offering a strategic advantage to growers. The synchronization of male and female floral functions not only optimizes fruit set and commercial quality but also presents a valuable framework for improving pollination efficiency under suboptimal conditions such rain-induced pollen washout[32,43,59]. These insights support a shift toward time-targeted pollination strategies, enabling effective supplementary pollination during early evening or morning hours when natural pollination may be delayed or ineffective.

Conclusion

The findings of this study provide practical, science-based insights which helped to propose the strategies (Supplementary Fig. 7) for optimizing pollination and extending the reproductive period in *S. undatus*. By leveraging environmental cues such as early summer rains and associated temperature shifts, we suggest that microclimate manipulation techniques—such as fogging, misting, sprinklers, shade management, and rain guns or temporary cost-effective greenhouse conditions—could potentially stimulate additional flowering cycles during long-day conditions without reliance on artificial lighting. Similarly, the identification of delayed autogamy and structural floral constraints in white-fleshed variety which belongs to *S. undatus* underscores the strong necessity of supplementary pollination, particularly cross-pollination, to achieve optimal fruit set and commercial-grade fruit size and weight. In addition, the field observations of pollen viability and stigma receptivity indicate a critical pollination window—between 4 h before and 12 h after anthesis—highlights the feasibility of manual pollination either evening and morning hours.

Collectively, these findings establish a validated framework linking reproductive biology to orchard-level management strategies, with direct implications for yield optimization in emerging dragon fruit production regions. However, given that the proposed strategies remain preliminary, further validation across locations and integration with additional climatic variables (temperature, humidity, solar radiation) will be essential for refining predictive models of floral induction and ensuring broad-scale adoption.

Materials and methods

Experimental site

The present study was conducted during 2023 and 2024 at H5 plot in the North Block orchard of the ICAR-National Institute of Abiotic Stress Management (NIASM), Baramati, India (18° 09' 30.62" N latitude, 74° 30' 03.08" E longitude, 570 m above mean sea level), falls within the Deccan Plateau Agroclimatic Zone (AZ-95) and Agroecological Region of AER-6. The study area experiences a hot and dry semi-arid climate, with an average annual rainfall of 560 mm, primarily from the south-west monsoon, classifying it as a water-scarce zone in Maharashtra, India. The mean maximum and minimum temperature of the region was 31.2 °C and 21.9 °C, respectively. The orchard was raised on degraded waste land featured by terrain of basaltic shallow soils[60].

Plant material

The present study was conducted at 10-year-old white-fleshed dragon fruit variety, NDFW-1 (NIASM Dragon Fruit White-1) belongs to *Selenicereus undatus* (Haw.) D. R. Hunt orchard established on pole system. The poles were installed at a spacing of 3.5 m between rows and 3.0 m between poles. Four plants were planted and trained on each pole using the mop-top system, and plants were raised with recommended practices[61]. The red-fleshed variety, NDFR-1 (NIASM Dragon Fruit Red-1) was used in the mode pollination experiment and also as a pollen source for cross-pollination. The later variety was maintained in dragon fruit diversity block established at ICAR-NIASM, Baramati.

Monitoring reproductive period and flowering cycles

The reproductive period of *S. undatus* (var. NDFW-1) was monitored over two consecutive years (2023–2024) under subtropical field conditions in India to characterize flowering seasonality, cycle frequency, and reproductive phenological stage durations. Observations were conducted on all cladodes of plants trained on 25 support poles, beginning two weeks before the spring equinox (21 March) and continuing until two weeks after the autumnal equinox (21 September), a period corresponding to the long-day photoperiod window that encompasses both the pre-monsoon summer (March–June) and the southwest monsoon season (June–September) in India. The reproductive period, or flowering season, was defined as the interval from the initiation of floral buds in the first flowering cycle of the year to the maturity of fruits from the final cycle. A flowering cycle was considered as the time from floral bud initiation to fruit maturity, and the total reproductive duration was determined by summing the lengths of all cycles observed in the season. At the onset of each cycle, 20 floral buds were randomly selected, tagged with aluminum labels, and marked with a permanent-coloured marker pens for traceability. These buds were monitored at regular intervals to record their progression through defined reproductive phenological stages: floral bud initiation, anthesis (flower opening and closing), fruit set, fruit development, and fruit maturity[62]. Two key developmental intervals—bud initiation to anthesis, and anthesis to fruit maturity—were measured for each marked bud, enabling detailed assessment of reproductive phenological durations across all flowering cycles.

Additional observations on the pattern of floral bud initiation during the spring (pre-monsoon) of 2025 were conducted at two locations, accompanied by supplementary rainfall data, to further support and validate the findings from 2023 to 2024.

Mode of pollination

To determine and clarify the mode of pollination in dragon fruit, two clones—viz., NDFW-1 and NDFR-1—were selected. These represent *S. undatus* (Haw.) D.R. Hunt and either *S. costaricensis*/*S. monacanthus* (Lemaire) D.R. Hunt or *S. polyrhizus* (F.A.C. Weber) Britton & Rose, respectively. The clones were grown in separate orchards and were reported to exhibit self-pollination and cross-pollination, respectively. Five sets of 20 flowers in both the clones were subjected to different pollination (Supplementary Figure. 1) treatments viz., bagging with wider wire net (BWNt), bagging with narrow wire net (BNNt), manual self-pollination (MSP), manual cross pollination (MCP), and open pollination (OP). The two treatments viz. BWNt and BNNt included to facilitate natural self-pollination, the former treatment restricting the insect pollinators but not wind whereas later one restricted both. In both the cases, wire network cages were used to avoid overweight of bags on flowers so that imposing

treatments should not interrupt natural pollination. MSP was done by pollinating the stigma of flowers manually using the pollens from the same flower in both clones. This was done by removing the entire perianth along with the attached stamens and gently rubbing the stigma twice in a back-and-forth motion against the anthers to ensure adequate and uniform pollen deposition (Supplementary Fig. 1A-D). MCP of NDFW-1 was performed by manually pollinating its flowers stigma with pollens from NDFR-1 and vice versa. After manual pollinations (MSP and MCP), the pollinated stigmas were covered with butter paper to prevent unintended pollination. In open pollination, the flowers were kept open and undisturbed allowing for natural pollination. After one month of pollination treatments, the fruits were counted upon maturity and their individual weights were recorded in gram (g). Ten individual fruits obtained as a result each different pollination were sliced, extracted the seed and counted them manually to determine the number of seeds per fruit.

The activity of floral visitors was monitored and documented photographically during the blooming period to assess the diversity of visitors and their potential role in pollination. Observations were conducted on approximately 100 flowers borne on both sides of two parallel rows comprising 10 support poles each (total of 20 poles). Monitoring was carried out for approximately 10 min at 1-hour intervals, beginning from flower opening at 19:00 h (on the day of anthesis) until floral senescence, indicated by bending of the perianth, at approximately 16:00 h the following day. Representative photographs of visiting insects were taken, and selected specimens were collected and submitted to an entomologist for identification. Recorded live video of a honey bee foraging on a dragon fruit flower.

Monitoring the anthesis and blooming patterns

Opening and closing of flowers in 20 bulged floral buds of NDFW-1 were monitored on the day of anthesis from 6:00 AM to 8:00 PM of following day, at one hour interval, during 6th cycle in each year to record timing and sequential phases of anthesis. The timing and duration of each bending phase were recorded and images were captured. The duration of flower opening was calculated by measuring the interval between the opening and closing of flower. Flowers were also monitored and captured images using DSLR camera (Canon) for measuring the bending intensity at every 2 h interval between 2 h before anthesis (BA) and 24 h after anthesis (AA). In the present study, 8:00 PM was considered the reference point as time of anthesis. All the marked flowers were monitored for recording the bending angle (direct/ribbon method) and to score bending intensity on a 0–4 scale[63].

Anther dehiscence

On the day of anthesis, five sets of 10 NDFW-1 floral buds each were monitored visually from 2:00 PM onwards hourly until 6.00 PM by opening the floral buds and observed under magnifying lens to confirm shedding of pollen from anthers. This was further confirmed by gently taping the floral tube and observe for pollen dust on petals.

Pollen viability test

The pollen viability was assessed by acetocarmine test[64]. To simplify the reference time, we identified 8:00 PM, when the flowers begin to bloom, as 0 h (0 h) and considered as the time of initiation of anthesis (AI) and before that as BA (before anthesis) and designated with negative sign (-). Similarly, the time period after 8:00 PM as considered as after anthesis (AA) and designated with positive sign (+). The pollen viability was tested at every 6 h interval from 12 h BA and 42 h AA.

Pollen grains displaying abnormal sizes/shape, pale color, or lacking/reduced protoplasm were classified as non-stained as compared to a well-defined exine and brightly stained protoplasm as stained. The percentage of pollen viability was calculated by.

$$\text{Pollen viability}(\%) = \frac{\text{No. of stained pollen}}{Total\ no.\ of\ pollen} \times 100$$

The pollen viability was also examined by adopting in vivo method[49] based on fruit setting (other fruit parameters therefrom) upon pollinating the different sets of receptive stigma (of 20 flowers in each set) with the pollens collected at different intervals 12 h before, and 42 after the reference anthesis time. The fruits thus formed were recorded for weight, length, diameter and number of seeds.

In vivo and in vitro pollen germination

In-vivo pollen germination was assessed via microscopic observation of germinating pollen on stigma lobes, which were pollinated at 6:00 PM (2 h BA). The stigma lobes were collected every two hours after pollination and taken to the laboratory, where they were gently squashed on a slide with the addition of acetocarmine stain for microscopic examination. For in vitro studies, pollens were collected at every 4 h intervals between 12 h before the anthesis (8:00 AM on the day anthesis) and 36 h after anthesis (8:00 AM on the next day of anthesis). The collected pollens were immediately incubated for germination in the medium containing 6 g/L of agar, 100 g/L of sucrose, 518 mg/L of calcium nitrate, and 636 mg/L of boric acid, with pH adjusted to 5.0, at room temperature of around 25°C[65]. Pollen grains were considered to have germinated when the pollen tube was at least twice the diameter of the grains. The germination percentage was calculated by dividing the number of germinated pollen grains observed in each field by the total number of pollen grains in that field[66]. In vitro pollen germination was validated via images of in vivo pollen germination.

Stigma receptivity

The receptivity of stigmas was assessed by hydrogen peroxide method[66,67] at every 6 h intervals between 48 h BA (−48 h) and AA (+ 48 h). For assessing the stigma receptivity prior to anthesis (−48 h to −6 h), selected 120 floral buds (8 sets of 15 floral buds each) and their stigma were directly subjected to hydrogen peroxide test assuming no self-pollination as there was no anther dehiscence. For assessing the stigma receptivity after anthesis (from 0 h to + 48 h), 135 flowers (9 sets of 15 flowers each) were emasculated and covered with butter paper bag to avoid natural out-crossing. A set of stigmas from floral buds or emasculated flowers were cut-off at every six hours, during above mentioned period and brought to the laboratory. Then, three stigma lobes from each floral bud or flower were immersed in approximately 15–20 ml of 6% hydrogen peroxide poured into a Petri dish for 3–4 min, and observed for bubbles formation using a macro lens. On the basis of intensity and size of bubbles, stigmas were classified as - no receptivity (-), very less receptivity (+), less receptivity (++), moderate receptivity (+++), high receptivity (++++), and very high receptivity (+++++).

The stigma receptivity was also examined by in vivo method[49] based on fruit setting upon pollinating the stigma of different sets (of 20 flowers in each set) of flowers at different intervals between 54 h before and 42 h after anthesis time (8:00 PM) using viable pollens. After 30 days of pollination, the fruits formed were used for recording weight, length, diameter and number seeds.

Data analysis

The data on duration of flowering cycle (anthesis to maturity) and time required for anthesis were subjected to analysis of variance (ANOVA), and treatment means were compared by Tukey test using R 4.4.2 version software with the grapesAgri1 package[68]. The data on pollination treatments, pollen germination, pollen viability (both in-vitro and in vivo), stigma receptivity based on in vivo fruit set was analyzed statistically by Kruskal Wallis Test, since the values were non-parametric in nature and treatment means were compared by Dunn's test[69]. The graphical effective pollination zones were drawn in Microsoft Excel based on pooled data of fruit set and fruit weight in the in vivo tests of pollen viability and stigma receptivity.

Data availability

The manuscript presents all the data generated in this research. Additional raw data will be shared upon request to the primary corresponding author ([bors_km@yahoo.co.in](mailto: bors_km@yahoo.co.in)).

Received: 5 July 2025; Accepted: 19 September 2025
Published online: 24 October 2025

References

1. Gonella, K., Nayak, S. P., Garg, M. & Kotebagilu, N. P. Impact of the COVID-19 pandemic on immune boosting food consumption and overall dietary pattern among selected Indian adults: an observational study. *Clin. Epidemiol. Glob Health*. **15**, 101056. https://doi.org/10.1016/j.cegh.2022.101056 (2022).
2. Vaillant, F., Perez, A., Davila, I., Dornier, M. & Reynes, M. Colorant and antioxidant properties of red-purple Pitahaya (*Hylocereus* sp). *Fruits* **60**, 3–12. https://doi.org/10.1051/fruits:2005007 (2005).
3. Ortiz-Hernandez, Y. D. *Hacia El Conocimiento Y conservación De La Pitahaya (Hylocereus spp)* (IPN-SIBEJ-CONACYT-FMCN, 2000).
4. Korotkova, N., Borsch, T. & Arias, S. A phylogenetic framework for the Hylocereeae (Cactaceae) and implications for the circumscription of the genera. *Phytotaxa* **327**, 1–46. https://doi.org/10.11646/phytotaxa.327.1.1 (2017).
5. Shah, K., Chen, J., Chen, J. & Qin, Y. Pitaya Nutrition, Biology, and biotechnology: A review. *Int. J. Mol. Sci.* **24**, 13986. https://doi.org/10.3390/ijms241813986 (2023).
6. Nobel, P. & de la Barrera, E. High temperatures and net CO2 Uptake, Growth, and stem damage for the hemiepiphytic cactus *Hylocereus Undatus*. *Biotropica* **34**, 225–231. https://doi.org/10.1646/0006-3606((2002). 2002)034[0225:HTANCU]2.0.CO;2.
7. Nobel, P. S. *Environmental Biology of Agaves and Cacti* (Cambridge Univ. Press, 1988). https://doi.org/10.21829/abm9.1990.1124
8. Nie, Q. et al. Isolation and characterization of a catalase gene HuCAT3 from Pitaya (*Hylocereus undatus*) and its expression under abiotic stress. *Gene* **563**, 63–67. https://doi.org/10.1016/j.gene.2015.03.007 (2015).
9. Wakchaure, G. C. et al. Long-term response of Dragon fruit (*Hylocereus undatus*) to transformed rooting zone of a shallow soil improving yield, storage quality and profitability in a drought-prone semi-arid agro-ecosystem. *Saudi J. Biol. Sci.* **30**, 103497. https://doi.org/10.1016/j.sjbs.2022.103497 (2023).
10. Karunakaran, G. et al. Promising high value fruit crops for Northeastern region. *Indian Hortic.* **68** (6), 35–39 (2023).
11. Nangare, D. et al. Dragon fruit: A potential crop for abiotic stressed areas. *NIASM Tech. Bull.* **47**, 24–pp (2020). ICAR-NIASM, Baramati, Maharashtra, India.
12. Wakchaure, G. C. et al. Dragon Fruit Cultivation in India: Scope, Constraints and Policy Issues. Technical Bulletin No. 27 ICAR-NIASM, Baramati, Pune, Maharashtra. (2021).
13. Eusebio, J. E. & Alaban, M. C. *Current status of dragon fruit and its prospects in the Philippines*. In FFTC Agricultural Policy Platform. Food and Fertilizer Technology Center for the Asian and Pacific Region. Retrieved August 15, 2025, from (2018)., June 29 https://ap.fftc.org.tw/article/1295
14. Raveh, E., Nerd, A. & Mizrahi, Y. Responses of two hemiepiphytic fruit-crop cacti to different degrees of shade. *Hortsci* **73**, 151–164. https://doi.org/10.1016/S0304-4238(97)00134-9 (1998).
15. Kakade, V. D. et al. Package of practices for cultivation of dragon fruit in multiple stressed areas. *Tech. bullet.* 32 (2025).
16. Mamaril, C. A. Isolation, identification and pathogenicity of organisms associated with dragon fruit (*Hylocereus undatus*, Haw.). *Unpubl. Thesis*, Cavite State University, Indang, Cavite (2010).
17. Tepora, T. F. Insect pests associated with dragon fruit (*Hylocereus undatus*, Haw Britton and Rose) in the Province of Cavite. *Unpubl. Res.*, Cavite State University, Indang, Cavite (2007).
18. Salunkhe, V. N., Bhagat, Y. S., Chavan, S. B., Lonkar, S. G. & Kakade, V. D. First report of *Neoscytalidium dimidiatum* causing stem canker of Dragon fruit (*Hylocereus* spp.) in India. *Plant. Dis.* **107** https://doi.org/10.1094/PDIS-04-22-0909-PDN (2022).
19. Karunakaran, G. & Arivalagan, M. Dragon fruit – a new introduction crop with promising market. *Indian Hortic.* **63**, 8–11 (2019).
20. Boraiah, K. M. et al. Enhancing the productivity of Dragon fruit through supplementary pollination. *ICAR-NIASM Tech. Folder* **52**, 6 (2022).
21. Boraiah, K. M. et al. Supplementary manual pollination: a potential technology to enhance the yield and quality in white fleshed Dragon fruit variety. *Natl. Acad. Sci. Lett.* **47**, 335–338. https://doi.org/10.1007/s40009-023-01356-2 (2024).

22. Macgregor, C. J. & Scott-Brown, A. S. Nocturnal pollination: an overlooked ecosystem service vulnerable to environmental change. *Emerg. Top. Life Sci.* **4**, 19–32. https://doi.org/10.1042/ETLS20190134 (2020).
23. Buxton, M. N., Gaskett, A. C., Lord, J. M. & Pattemore, D. E. A global review demonstrating the importance of nocturnal pollinators for crop plants. *J. Appl. Ecol.* **59**, 2890–2901. https://doi.org/10.1111/1365-2664.14284 (2022).
24. Klatt, B. K. et al. Bee pollination improves crop quality, shelf life and commercial value. *Philos. Trans. R Soc. B Biol. Sci.* **281** (1775), 20132440. https://doi.org/10.1098/rspb.2013.2440 (2013).
25. Wietzke, A. et al. Pollination as a key factor for strawberry fruit physiology and quality. *Ber Jul Kühn-Institut.* **183**, 49 (2016).
26. Hopping, M. E. & Hacking, N. J. A comparison of pollen application methods for the artificial pollination of Kiwifruit. *Acta Hortic.* **139**, 41–50. https://doi.org/10.17660/ActaHortic.1983.139.5 (1983).
27. Tacconi, G., Michelotti, V., Cacioppo, O. & Vittone, G. Kiwifruit pollination: the interaction between pollen quality, pollination systems and flowering stage. *J. Berry Res.* **6**, 417–426. https://doi.org/10.3233/JBR-160138 (2016).
28. Joanna, C. L. Y. & Ding, P. Floral morphology and pollination process of red-fleshed Dragon fruit (*Hylocereus polyrhizus*) grown in an open field. *Hortic. Sci. Technol.* **39**, 277–293. https://doi.org/10.7235/HORT.20210025 (2021).
29. Rech, A. R. et al. *Biologia Da Polinização*528 (Editora Projeto Cultural, 2014).
30. Valiente-Banuet, A. Pollination biology of the hemiepiphytic cactus *Hylocereus Undatus* in the Tehuacán Valley, Mexico. *J. Arid Environ.* **68**, 1–8. https://doi.org/10.1016/j.jaridenv.2006.04.001 (2007).
31. Chu, Y. C. & Chang, J. C. Codification and description of the phenological growth stages of red-fleshed Pitaya (*Hylocereus polyrhizus*) using the extended BBCH scale – with special reference to spines, areole, and flesh color development under field conditions. *Sci. Hortic.* **293**, 110752. https://doi.org/10.1016/j.scienta.2021.110752 (2022).
32. Muniz, J. P. O., Bomfim, I. G. A., Corrêa, M. C. M. & Freitas, B. M. Floral biology, pollination requirements and behavior of floral visitors in two species of Pitaya. *Rev. Ciênc Agron.* **50**, 640–649. https://doi.org/10.5935/1806-6690.20190076 (2019).
33. Weiss, J., Nerd, A. & Mizrahi, Y. Flowering and pollination requirements in climbing cacti with fruit crop potential. *Hortic. Sci.* **29**, 1487–1492. https://doi.org/10.21273/HORTSCI.29.12.1487 (1994).
34. Le Bellec, F. Pollinisation et fécondation d'*Hylocereus Undatus* et d'*H. Costaricensis* à l'île de La Réunion. *Fruits* **59**, 411–422. https://doi.org/10.1051/fruits:2005003 (2004).
35. Wilkie, J. D., Sedgley, M. & Olesen, T. Regulation of floral initiation in horticultural trees. *J. Exp. Bot.* **59** (12), 3215–3228. https://doi.org/10.1093/jxb/ern188 (2008).
36. Xiong, R. et al. Transcriptomic analysis of flower induction for long-day Pitaya by supplementary lighting in short-day winter season. *BMC Genom.* **21**, 329. https://doi.org/10.1186/s12864-020-6726-6 (2020).
37. Devi, P. et al. Studies on the floral behavior of Dragon fruit (*Hylocereus costaricensis*) and their qualitative characters. *Environ. Ecol.* **41**, 174–179 (2023).
38. Dhiman, S., Adhikary, T., Brar, J. S. & Chand, K. Unveiling the secrets of dragon fruit flowering. *Just Agric.* 4(12), e-ISSN: 2582–8223 (2024).
39. Rashid, S. H. S., Azam, G. & Chowdhury, S. Influence of day-length enhancement through night-breaking by artificial lighting on off-season Dragon fruit production. *Asian J. Adv. Agric. Res.* **17**, 1–10. https://doi.org/10.9734/AJAAR/2021/v17i230190 (2021).
40. N'Guyen, Q. T., Ngo, M. D., Truong, T. H., Nguyen, D. C. & N'Guyen, M. C. Modified compact fluorescent lamps improve light-induced off-season floral stimulation in Dragon fruit farming. *Food Sci. Nutr.* **9**, 2390–2401. https://doi.org/10.1002/fsn3.2088 (2021).
41. Morales Peña, V. H. et al. The phenology of coffea Arabica var. Esperanza L4A5 under different agroforestry associations and fertilization conditions in the Caribbean region of Costa Rica. *Agriculture* **14**, 1988. https://doi.org/10.3390/agriculture14111988 (2024).
42. Pushpakumara, D. K. N. G., Gunasena, H. P. M. & Karyawasam, M. Flowering and fruiting phenology, pollination vectors and breeding system of Dragon fruit (*Hylocereus* spp). *Sri Lankan J. Agric. Sci.* **42**, 81–91 (2005).
43. Tran, D. H. & Yen, C. R. Morphological characteristics and pollination requirement in red Pitaya (*Hylocereus* spp). *Int. J. Biol. Biomol. Agric. Food Biotechnol. Eng.* **8**, 202–206 (2014). https://api.semanticscholar.org/CorpusID:13372088
44. Mizrahi, Y., Nerd, A. & Sitrit, Y. New fruits for arid climates. In *New Trends in New Crops and New Uses* (eds Janick, J. & Whipkey, A.) 378–384 (ASHS, 2002).
45. Marques, V. B., Moreira, R. A., Ramos, J. D., Araújo, N. A. & Silva, F. O. R. Fenologia reprodutiva de Pitaia Vermelha no município de Lavras, MG. *Ciênc Rural.* **41** (6). https://doi.org/10.1590/S0103-84782011005000071 (2011).
46. Castillo, M. R. & Ortiz, Y. D. Floración y fructificación de Pitajaya En Zaachila, Oaxaca. *Rev. Fitotec Mexicana*. **17**, 12–19. https://doi.org/10.35196/rfm.1994.1.12 (1994).
47. Luu, T. T., Le, T. L., Huynh, N. & Quintela-Alonso, P. Dragon fruit: A review of health benefits and nutrients and its sustainable development under climate changes in Vietnam. *Czech J. Food Sci.* **39**, 57–69. https://doi.org/10.17221/139/2020-CJFS (2021).
48. Li, J. C., Dai, H. F. & Sun, Q. M. Breeding report of a new Pitaya cultivar Hongshuijing 6. *J. Fruit Sci.* **39**, 1973–1976. https://doi.org/10.13925/j.cnki.gsxb.20220176 (2022).
49. Li, J. et al. Pollen germination and hand pollination in Pitaya (*Selenicereus* spp). *Emir J. Food Agric.* **34**, 369–387. https://doi.org/10.9755/ejfa.2022.v34.i5.2855 (2020).
50. Lichtenzveig, J., Abbo, S., Nerd, A., Tel-Zur, N. & Mizrahi, Y. Cytology and mating system in the climbing cacti *Hylocereus* and *Selenicereus*. *Am. J. Bot.* **87**, 1058–1065. https://doi.org/10.2307/2657005 (2000).
51. Cohen, H. & Tel-Zur, N. Morphological changes and self-incompatibility breakdown associated with autopolyploidization in *Hylocereus* species (Cactaceae). *Euphytica* **184** (3), 345–354. https://doi.org/10.1007/s10681-011-0536-5 (2011).
52. Zhang, T. et al. Genetic analyses of flower main traits from two Pitayas and their progenies: a cactus plant. *Plants* **13** (5), 699. https://doi.org/10.3390/plants13050699 (2024).
53. Bustamante, E., Casas, A. & Búrquez, A. Geographic variation in reproductive success of stenocereus thurberi (Cactaceae): effects of pollination timing and pollinator guild. *Am. J. Bot.* **97** (12), 2020–2030. https://doi.org/10.3732/ajb.1000071 (2010).
54. Boraiah, K. M. et al. Prevention of flower drop in Dragon fruit through bagging, sheltering and supplementary pollination. *ICAR-NIASM Tech. Folder* **51**, 6 (2021).
55. Fenster, C. & Martén-Rodríguez, S. Reproductive assurance and the evolution of pollination specialization. *Int. J. Plant. Sci.* **168**, 215–228. https://doi.org/10.1086/509647 (2007).
56. Del Pérez, A., Garay, A. L. A., Rivera, A. V. & Gutiérrez, R. G. Y. & Preciado Rangel, P. Elements to improve the management and commercialization of dragon fruit (*Hylocereus undatus* (Haworth) D.R. Hunt). *Agro Productividad* (2023). https://doi.org/10.32854/agrop.v16i2.2381
57. Egea, J., Burgos, L., Garcia, J. E. & Egea, L. Stigma receptivity and style performance in several apricot cultivars. *J. Hortic. Sci.* **66**, 19–25. https://doi.org/10.1080/00221589.1991.11516120 (1991).
58. Herrero, M. & Arbeloa, A. Influence of the pistil on pollen-tube kinetics in Peach (*Prunus persica*). *Am. J. Bot.* **76**, 1441–1447. https://doi.org/10.1002/j.1537-2197.1989.tb15124.x (1989).
59. Moreira, R. A. et al. Natural and artificial pollination of white-fleshed Pitaya. *Acad. Bras. Ciênc.* **94** (suppl.3). https://doi.org/10.1590/0001-3765202220211200 (2022). e20211200.
60. Minhas, P. S. et al. Turning basaltic terrain into model research farm: Chronicle description. *NIASM Tech. Bull.* 8, ICAR-NIASM, Baramati, Pune, India, 64 pp. (2015). https://doi.org/10.13140/RG.2.1.3027.3444
61. Kakade, V. D. et al. Emerging technologies for enhancing the productivity and quality of Dragon fruit. *ICAR-NIASM Tech. Folder.* **56**, 12 (2023).

62. Kishore, K. Phenological growth stages of Dragon fruit (*Hylocereus undatus*) according to the extended BBCH scale. *Sci. Hort.* **213**, 294–302. https://doi.org/10.1016/j.scienta.2016.10.047 (2016).
63. Boraiah, K. M. et al. Identification and measurement of flower bending in Dragon fruit. *ICAR-NIASM Tech. Folder* **77**, 6 (2025).
64. Pio, L. A. S. et al. M. Viabilidade do pólen de Laranjas Doces Em diferentes condições de Armazenamento. *Ciênc Agrotec.* **31**, 147–153. https://doi.org/10.1590/S1413-70542007000100022 (2007).
65. Fagundes, M. C. P., Ramos, J. D., Tostes, N. V., Pasqual, M. & Rodrigues, F. A. In vitro germination of pollen grains in Pitahaya species. *Int. J. Fruit Sci.* **21**, 556–564. https://doi.org/10.1080/15538362.2021.1913469 (2021).
66. Kearns, C. A. & Inouye, D. W. *Techniques for Pollination Biologists* (University Press of Colorado, 1993).
67. Zeisler, M. Über die abgrezung des Eigentlichen Narbenflüche Mit Hilfe von reaktionen. *Beittr Bot. Zenti V*. **58**, 308–318 (1993).
68. Gopinath, P. P., Parsad, R., Joseph, B. & Adarsh, V. S. GrapesAgri1: collection of Shiny apps for data analysis in agriculture. *J. Open. Source Softw.* **6**, 3437 (2021). https://www.kaugrapes.com/home
69. Gopinath, P. P., Parsad, R., Joseph, B. & Adarsh, V. S. GRAPES: General Rshiny Based Analysis Platform Empowered by Statistics (2020). https://www.kaugrapes.com/home

Acknowledgements
We sincerely thank the staff of ICAR-National Institute of Abiotic Stress Management, who helped throughout this research work.

Author contributions
BKM, JR, HP: conceptualization, designed the experiment and editing; PJ: carried out the research (lab and field experiments) and drafted the manuscript; BKM, PJ, PK: contributed to data acquisition and analysis; KSR, HP: monitoring and guidance during experiment; SSD, KKP, VDK, BSP, HCB, HMH, DBK, SAR, JR, HP: edited and validated the final version of the manuscript. All authors reviewed the manuscript and approved it for submission.

Funding
This research received no specific grant from any funding agency in the public, commercial or not-for-profit sectors. However, the research was supported by the Indian Council of Agricultural Research, Department of Agricultural Research and Education, Government of India.

Declarations

Competing interests
The authors declare no competing interests.

Additional information
Supplementary Information The online version contains supplementary material available at https://doi.org/10.1038/s41598-025-21168-2.

Correspondence and requests for materials should be addressed to K.M.B.

Reprints and permissions information is available at www.nature.com/reprints.

Publisher's note Springer Nature remains neutral with regard to jurisdictional claims in published maps and institutional affiliations.

Open Access This article is licensed under a Creative Commons Attribution-NonCommercial-NoDerivatives 4.0 International License, which permits any non-commercial use, sharing, distribution and reproduction in any medium or format, as long as you give appropriate credit to the original author(s) and the source, provide a link to the Creative Commons licence, and indicate if you modified the licensed material. You do not have permission under this licence to share adapted material derived from this article or parts of it. The images or other third party material in this article are included in the article's Creative Commons licence, unless indicated otherwise in a credit line to the material. If material is not included in the article's Creative Commons licence and your intended use is not permitted by statutory regulation or exceeds the permitted use, you will need to obtain permission directly from the copyright holder. To view a copy of this licence, visit http://creativecommons.org/licenses/by-nc-nd/4.0/.

© The Author(s) 2025